International Journal of Bifurcation and Chaos, Vol. 19, No. 10 (2009) 3445–3459
© World Scientific Publishing Company

Int. J. Bifurcation Chaos 2009.19:3445-3459. Downloaded from www.worldscientific.com
by UNIVERSIDAD DE CHILE SISTEMA DE SERVICIOS DE INFORMACION Y BIBLIOTECAS (SISIB) on 03/20/13. For personal use only.

GENERATION AND CHARACTERIZATION OF ABSOLUTE EQUILIBRIUM OF COMPRESSIBLE FLOWS

GIORGIO KRSTULOVIC, CARLOS CARTES and MARC BRACHET
Laboratoire de Physique Statistique de l'Ecole Normale Supérieure, associé au CNRS et aux Universités Paris VI et VII, 24 Rue Lhomond, 75231 Paris, France

ENRIQUE TIRAPEGUI
Departamento de Física, Facultad de Ciencias Físicas y Matemáticas de la Universidad de Chile, Blanco Encalada 2008, Santiago, Chile

Received June 1, 2008; Revised December 13, 2008

A short review is given of recent papers on the relaxation to (incompressible) absolute equilibrium. A new algorithm to construct absolute equilibrium of spectrally truncated compressible flows is described. The algorithm uses stochastic processes based on the Clebsch representation of the velocity field to generate density and velocity fields that follow by construction the absolute equilibrium stationary probability. The new method is shown to reproduce the well-known Gaussian results in the incompressible limit. The irrotational compressible absolute equilibrium case is characterized and the distribution is shown to be non-Gaussian. The high-temperature compressible spectra are found not to obey k^2 scaling. Finally, oscillating behavior in constant-pressure variable-temperature relaxation is obtained, suggesting the presence of second sound.

Keywords: Truncated Euler equation; Clebsch potentials; compressible fluids; relaxation.

1. Introduction

It is well-known [Lee, 1952; Kraichnan, 1973; Orszag, 1977] that the (inviscid and conservative) incompressible Euler equation (Galerkin) truncated by keeping only a finite number of spatial Fourier harmonics admits absolute equilibrium solutions with Gaussian statistics, equipartition of kinetic energy among all Fourier modes and thus an energy spectrum $E(k) \sim k^2$.

A recent series of papers [Cichowlas *et al.*, 2005; Bos & Bertoglio, 2006; Krstulovic & Brachet, 2008; Krstulovic *et al.*, 2009; Frisch *et al.*, 2008], focusing on the dynamics of convergence toward absolute equilibrium, revived the interest in these matters by producing new and unexpected results. It was found in particular that in this time-reversible system (long-lasting) transients are obtained that mimic (irreversible) viscous flows.

The purpose of this paper is to extend these recent results to compressible flows. The absolute equilibrium is Gaussian in the case of incompressible flows, because the conserved quantities (energy and helicity) are quadratic. In the case of compressible flows the conserved quantities are not quadratic and the corresponding stationary probability is thus non-Gaussian. It is therefore a nontrivial problem to generate such a compressible absolute equilibrium flow.

The main result of this paper is a new algorithm to generate compressible absolute equilibrium.

Int. J. Bifurcation Chaos 2009.19:3445-3459. Downloaded from www.worldscientific.com
by UNIVERSIDAD DE CHILE SISTEMA DE SERVICIOS DE INFORMACION Y BIBLIOTECAS (SISIB) on 03/20/13. For personal use only.

We use the Hamiltonian Clebsch representation of the velocity field to generate density and velocity fields that follow by construction the absolute equilibrium stationary probability.

The paper is organized as follows: in Sec. 2 we give a short review of the recent series of papers on the dynamics of convergence toward absolute equilibrium in the incompressible case. In this section, we also review several early papers related to the compressible dynamics. Although these papers do not explicitly refer to absolute equilibrium, they implicitly do so by introducing wave turbulence theory with ultraviolet cutoff. An explicit example of relaxation toward equilibrium in the compressible case is then given in Sec. 3. Our new algorithm is detailed in Sec. 4. In Sec. 5, numerical simulations are presented, first the algorithm is verified in the incompressible case and then the compressible absolute equilibria are studied. Preliminary results relating to the presence of second sound in constant pressure variable temperature relaxation are given in Sec. 6. Finally Sec. 7 is our conclusion.

2. A Short Review on Truncated Euler

This section contains a short review of the recent papers on the dynamics of convergence toward absolute equilibrium in the incompressible case. We will also review several early papers related to the compressible dynamics. These papers do not explicitly refer to absolute equilibrium, however, they implicitly do so by introducing wave turbulence theory with an explicit ultraviolet cutoff that is mandatory to make the theory finite.

2.1. *Basic definitions*

The truncated incompressible Euler equation is a finite system of ordinary differential equations for the complex variables $\hat{\mathbf{u}}(\mathbf{k})$ ($\mathbf{k}$ is a 3D vector of relative integers (k_1, k_2, k_3) satisfying $\sup_\alpha |k_\alpha| \leq k_{\max}$)

$$\partial_t \hat{u}_\alpha(\mathbf{k}, t) = -\frac{i}{2} \mathcal{P}_{\alpha\beta\gamma}(\mathbf{k}) \sum_{\mathbf{p}} \hat{u}_\beta(\mathbf{p}, t) \hat{u}_\gamma(\mathbf{k} - \mathbf{p}, t) \tag{1}$$

where $\mathcal{P}_{\alpha\beta\gamma} = k_\beta P_{\alpha\gamma} + k_\gamma P_{\alpha\beta}$ with $P_{\alpha\beta} = \delta_{\alpha\beta} - k_\alpha k_\beta / k^2$ and the convolution in (1) is truncated to $\sup_\alpha |k_\alpha| \leq k_{\max}$, $\sup_\alpha |p_\alpha| \leq k_{\max}$ and $\sup_\alpha |k_\alpha - p_\alpha| \leq k_{\max}$.

This system is classically obtained [Orszag, 1977] from the (unit density) three-dimensional incompressible Euler equation

$$\partial_t \mathbf{u} + (\mathbf{u} \cdot \nabla)\mathbf{u} = -\nabla p \tag{2}$$

$$\nabla \cdot \mathbf{u} = 0 \tag{3}$$

by performing a Galerkin truncation ($\hat{\mathbf{u}}(\mathbf{k}) = 0$ for $\sup_\alpha |k_\alpha| > k_{\max}$) on the Fourier transform $\mathbf{u}(\mathbf{x}, t) = \sum \hat{\mathbf{u}}(\mathbf{k}, t) e^{i\mathbf{k}\cdot\mathbf{x}}$ of the spatially periodic velocity field $\mathbf{u}$.

This time-reversible system exactly conserves the energy $E = \sum_k E(k, t)$ and helicity $H = \sum_k H(k, t)$, where the energy and helicity spectra $E(k, t)$ and $H(k, t)$ are defined by

$$E(k, t) = \frac{1}{2} \sum_{k - \Delta k/2 < |\mathbf{k}'| < k + \Delta k/2} |\hat{\mathbf{v}}(\mathbf{k}', t)|^2 \tag{4}$$

$$H(k, t) = \sum_{k - \Delta k/2 < |\mathbf{k}'| < k + \Delta k/2} \hat{\mathbf{u}}(\mathbf{k}', t) \cdot \hat{\omega}(-\mathbf{k}', t) \tag{5}$$

with spherical shells of width $\Delta k = 1$.

2.2. *Incompressible flows*

Cichowlas *et al.* [2005], Cichowlas [2005] observed that the incompressible Euler equation, (Galerkin) truncated as in (1) using a large spectral truncation wavenumber $k_{\max}$, displays long-lasting transients behaving just like high-Reynolds number viscous flow. In particular, they found an approximately $k^{-5/3}$ inertial range followed by a dissipative range. Such a behavior is possible because the highest-k modes thermalize at first, through a mechanism discovered by Lee [1952], leading to a k^2 spectrum. Progressively the thermalized region extends to lower and lower wavenumbers, eventually covering the whole range of available modes. At intermediate times, when the thermalized regime only extends over the highest wavenumbers, it acts as a thermostat that pumps out the energy of larger-scale modes. The energy spectrum for different values of $k_{\max}$ and its temporal evolution taken from [Cichowlas, 2005] are shown in Fig. 1. In this context, the spectrally truncated Euler equations appeared as a minimal model of turbulence.

Bos and Bertoglio [2006] studied the evolution of the turbulent energy spectrum for the inviscid spectrally truncated Euler equations using Eddy-Damped Quasi-Normal Markovian (EDQNM) closure calculations. They observed that the EDQNM

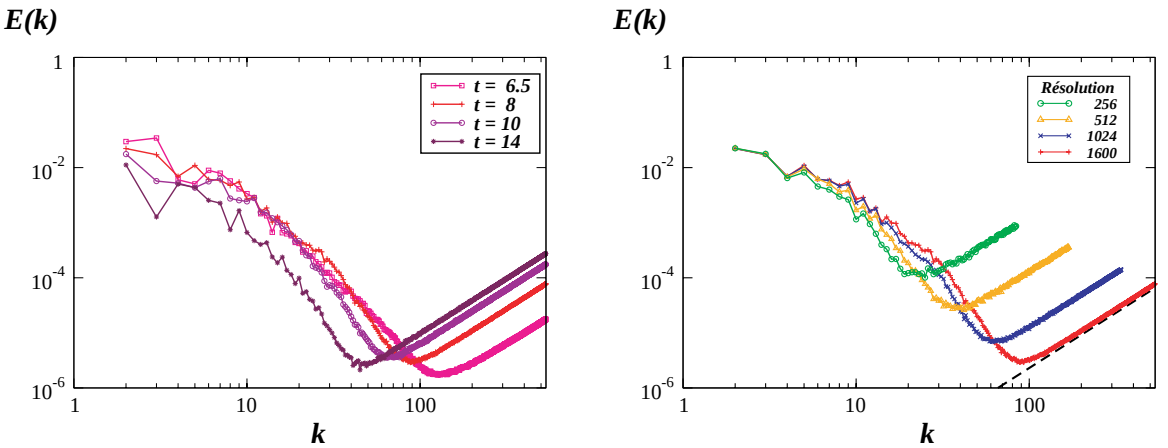

Fig. 1. Energy spectra, left: resolution 1600^3 at $t = (6.5, 8, 10, 14)$ ($\diamond$, $+$, $\circ$, $*$); right: resolutions 256^3 (circle $\circ$), 512^3 (triangle $\triangle$), 1024^3 (cross $\times$) and 1600^3 (cross $+$) at $t = 8$. The dashed lines indicate k^2 scaling. Figure taken from [Cichowlas, 2005].

closure reproduced the behavior found in the direct numerical simulations of reference [Cichowlas *et al.*, 2005]. They showed that the dissipation range was created by nonlinear interactions with the modes in equipartition. They defined a nonlocal effective eddy viscosity, based on the most energetic modes in the equipartition zone and the cutoff wave number.

Krstulovic and Brachet [2008] proposed a phenomenological two-fluid model of the (time-reversible) spectrally-truncated 3D Euler equation. They showed that the thermalized small scales follow a quasi-normal distribution. They determined the effective viscosity and thermal diffusion, using EDQNM closure and Monte-Carlo numerical computations, yielding compatible values. (Hypo)diffusion of heat was obtained using Monte Carlo and the corresponding effective Prandtl number was found to vanish in the small $k/k_{\max}$ limit. Overall, the phenomenological two-fluid model was found to be in good quantitative agreement with the original truncated Euler equations.

Krstulovic *et al.* [2008] studied for the first time the relaxation toward a Kraichnan [1973] helical absolute equilibrium. They found transient mixed energy and helicity cascades and used the concept of eddy viscosity, as previously developed in [Cichowlas *et al.*, 2005] and [Krstulovic & Brachet, 2008], to qualitatively explain the differences observed between truncated Euler and high-Reynolds number (fixed viscosity) Navier–Stokes. They finally showed that the truncated Euler large scale modes quantitatively follow an effective Navier–Stokes dynamics based on a (time and wavenumber dependent) eddy viscosity that did not depend explicitly on the helicity content in the flow.

Frisch *et al.* [2008] showed that the use of a high power α of the Laplacian in the dissipative term of hydrodynamical equations leads asymptotically to truncated inviscid *conservative* dynamics with a finite range of spatial Fourier modes. They found that, just as in reference [Cichowlas *et al.*, 2005], the modes at large wavenumbers thermalize, whereas modes at small wavenumbers obey ordinary viscous dynamics. They interpreted the energy bottleneck observed for finite α as incomplete thermalization.

2.3. *Compressible flows*

Putterman and Roberts [1982, 1983] investigated the solution to nonlocal dispersive classical hydrodynamics at the fourth order of nonlinearity. An extra degree of freedom appeared as a result of the additive conservation of wave number in the interaction of beams of sound waves, representing a broken symmetry. Imposing an ultraviolet cutoff to obtain finite results, they found that the resulting nonlinear high-order equations of motion for the background plus a distribution of sound waves were identical to the Landau two-fluid hydrodynamics used to describe superfluid Helium.

Larraza and Putterman [1986] showed that if a nonlinear medium is pumped with energy, in the form of mechanical waves, sufficiently far from equilibrium the wave turbulence can support a transition from diffusive to propagative energy transport that bears deep similarities to second sound in Helium.

Int. J. Bifurcation Chaos 2009.19:3445-3459. Downloaded from www.worldscientific.com
by UNIVERSIDAD DE CHILE SISTEMA DE SERVICIOS DE INFORMACION Y BIBLIOTECAS (SISIB) on 03/20/13. For personal use only.

Int. J. Bifurcation Chaos 2009.19:3445-3459. Downloaded from www.worldscientific.com
by UNIVERSIDAD DE CHILE SISTEMA DE SERVICIOS DE INFORMACION Y BIBLIOTECAS (SISIB) on 03/20/13. For personal use only.

Connaughton *et al.* [2005] studied the formation of a large-scale coherent structure (a condensate) in classical wave equations by considering the defocusing nonlinear Schrodinger equation as a representative model. They formulated a thermodynamic description of the classical condensation process by using a wave turbulence theory with ultraviolet cutoff. They found a subcritical condensation process in 3D, and no transition in 2D. Numerical simulations of the NLS equation with stochastic initial conditions were found to be in quantitative agreement with the equilibrium distribution of the kinetic equation derived from the NLS equation.

3. Relaxation in Compressible Spectrally Truncated Euler Flows

In this section, we study the relaxation to equilibrium of irrotational compressible spectrally truncated Euler flows. The dynamics is described by a density field ρ and the velocity $\mathbf{u}$ that is represented by the velocity potential ϕ. The dynamics is given by the continuity and Bernoulli equations:

$$\frac{\partial \rho}{\partial t} = -\nabla \cdot (\rho \nabla \phi) \tag{6}$$

$$\frac{\partial \phi}{\partial t} = -\frac{1}{2}\mathbf{u}^2 - \frac{\partial \varepsilon}{\partial \rho}(\rho) \tag{7}$$

$$\mathbf{u} = \nabla \phi \tag{8}$$

$$\varepsilon(\rho) = \frac{1}{2c^2}(\rho - 1)^2 \tag{9}$$

where $\varepsilon(\rho)$ is the internal energy of the fluid and c the speed of sound, when $\rho = 1$.

This time-reversible system ($t \to -t, \phi \to -\phi$) conserves the total mass, the momentum and the total energy:

$$Q = \int d^d x \rho(x,t) \tag{10}$$

$$\mathbf{P} = \int d^d x \rho(x,t) \nabla \phi(x,t) \tag{11}$$

$$H = \int d^d x \left[\frac{1}{2} \rho(x,t) \nabla \phi(x,t)^2 + \varepsilon(\rho) \right]. \tag{12}$$

As done in the incompressible case in [Cichowlas *et al.*, 2005; Krstulovic *et al.*, 2009] we now study the Galerkin truncated version of Eqs. (6)–(8) for the Fourier transforms $\hat{\rho}(\mathbf{k},t) \equiv \hat{\rho}_{\mathbf{k}}(t)$ and $\hat{\phi}(\mathbf{k},t) \equiv \hat{\phi}_{\mathbf{k}}(t)$ of the dynamical variables. This spectrally truncated system reads

$$\frac{\partial \hat{\rho}_{\mathbf{k}}}{\partial t}(t) = \sum_{\mathbf{p}} \hat{\rho}_{\mathbf{k}-\mathbf{p}}(t) \hat{\phi}_{\mathbf{p}}(t) \mathbf{k} \cdot \mathbf{p} \tag{13}$$

$$\frac{\partial \hat{\rho}_{\mathbf{k}}}{\partial t}(t) = \frac{1}{2} \sum_{\mathbf{p}} \hat{\phi}_{\mathbf{k}-\mathbf{p}}(t) \hat{\phi}_{\mathbf{p}}(t) (\mathbf{k} - \mathbf{p}) \cdot \mathbf{p} + \frac{1}{c^2} \widehat{(1-\rho)}_{\mathbf{k}}(t) \tag{14}$$

where the convolution in Eqs. (13) and (14) are truncated to $\sup_\alpha |k_\alpha| \le k_{\max}$, $\sup_\alpha |p_\alpha| \le k_{\max}$ and $\sup_\alpha |k_\alpha - p_\alpha| \le k_{\max}$. This system also exactly conserves Q, P and H.

Let us now define, as in the incompressible case (4), the internal, kinetic and total energy spectra by,

$$E_{\text{kin}}(k,t) = \frac{1}{2} \sum_{k - \frac{\Delta k}{2} < |\mathbf{k}'| < k + \frac{\Delta k}{2}} \widehat{\rho \mathbf{u}}_{-\mathbf{k}'}(t) \cdot \widehat{\mathbf{u}}_{\mathbf{k}'}(t) \tag{15}$$

$$E_{\text{int}}(k,t) = \frac{c^2}{2} \sum_{k - \frac{\Delta k}{2} < |\mathbf{k}'| < k + \frac{\Delta k}{2}} |\widehat{(\rho - 1)}_{\mathbf{k}'}|^2(t) \tag{16}$$

$$E(k,t) = E_{\text{kin}}(k,t) + E_{\text{int}}(k,t) \tag{17}$$

By construction we have $H = \sum_k E(k,t)$. Note that the systems (13) and (14) (as well as (6)–(8)) possesses a Hamiltonian structure. Equations (13) and (14) can thus be rewritten using the Hamiltonian

$$H = \sum_{\mathbf{k}} \frac{1}{2} \widehat{\rho \mathbf{u}}_{\mathbf{k}} \widehat{\mathbf{u}}^*_{\mathbf{k}} + \frac{1}{2c^2} |\widehat{(\rho - 1)}_{\mathbf{k}}|^2 \tag{18}$$

as the canonical equations

$$\frac{\partial \hat{\rho}_{\mathbf{k}}}{\partial t}(t) = \frac{\partial H}{\partial \hat{\phi}^*_{\mathbf{k}}}, \quad \frac{\partial \hat{\phi}^*_{\mathbf{k}}}{\partial t}(t) = -\frac{\partial H}{\partial \hat{\rho}_{\mathbf{k}}}, \tag{19}$$

where $\hat{\rho}_{\mathbf{k}}, \hat{\phi}^*_{\mathbf{k}}$ are thus conjugate variables.

As in incompressible truncated Euler, this system admits a stationary statistical solution with a probability distribution function given by $P\{\hat{\rho}_{\mathbf{k}}, \hat{\phi}_{\mathbf{k}}\} \sim e^{-\beta H}$. As H is not quadratic, the p.d.f. will not be Gaussian and no equipartition can be expected in the energy spectrum (17) because of the correlation between $\hat{\rho}_{\mathbf{k}}$ and $\hat{\phi}_{\mathbf{k}}$ for different wavenumbers. However, rewriting $\hat{\rho}_{\mathbf{k}} = 1 + \hat{\rho}'_{\mathbf{k}}$, the Hamiltonian can be written as $H = H_{\mathbf{G}} + H_{\mathbf{NG}}$

Int. J. Bifurcation Chaos 2009.19:3445-3459. Downloaded from www.worldscientific.com
by UNIVERSIDAD DE CHILE SISTEMA DE SERVICIOS DE INFORMACION Y BIBLIOTECAS (SISIB) on 03/20/13. For personal use only.

with

$$H_{\mathbf{G}} = \sum_{\mathbf{k}} \frac{1}{2} k^2 |\hat{\phi}_{\mathbf{k}}|^2 + \frac{1}{2c^2} |\hat{\rho}'_{\mathbf{k}}|^2 \tag{20}$$

$$H_{\mathbf{NG}} = \sum_{\mathbf{k}} \frac{1}{2} \widehat{\rho' \mathbf{u}}_{\mathbf{k}} \widehat{\mathbf{u}}^*_{\mathbf{k}}. \tag{21}$$

Note that for large values of β, $H_{\mathbf{NG}}$ can be safely neglected and statistics becomes Gaussian and equipartition, yielding in this limit $E(k) \sim k^2$ (in three dimensions).

It is well known that a conservative nonlinear systems with a high number of freedom degrees may, in general, not relax to an equilibrium state and time periodic localized structures can appear, as in the classical Fermi–Pasta–Ulam–Tsingou problem [Fermi *et al.*, 1955]. In order to study the relaxation to the equilibrium of truncated irrotational compressible flows and avoid long transient we will use an initial condition, close to the equilibrium state, given by a Gaussian field perturbed by a large-scale modulation of the velocity potential. This initial condition reads

$$\rho_0(x, y, z) = 1 + \rho'_{\mathrm{G}}(x, y, z) \tag{22}$$

$$\phi(x, y, z) = \frac{1}{8\sqrt{3}} (\sin 4x + \sin 4y + \sin 4z) + \phi_{\mathrm{G}}(x, y, z) \tag{23}$$

where $\hat{\rho}'_{\mathrm{G}\mathbf{k}}, \hat{\phi}_{\mathrm{G}\mathbf{k}}$ are distributed with a probability proportional to $e^{-\beta H_{\mathrm{G}}}$.

Numerical solutions of Eqs. (13) and (14) are efficiently produced using a standard pseudo-spectral general-periodic code with 128^3 Fourier modes that is dealiased using the 2/3 rule [Gottlieb & Orszag, 1977] by a Galerkin truncation at $k_{\max} = 42$. The numerical method used is nondispersive and conserves mass, momentum and energy with high accuracy. The value of β is chosen large enough to ensure that there are no points with negative ρ. The total initial energy (18) of this run is $H = 2.136$.

Figure 2 shows the temporal evolution of the energy spectrum. Note that the system effectively relaxes but at the final time $t = 43.69$ in Fig. 2(d),

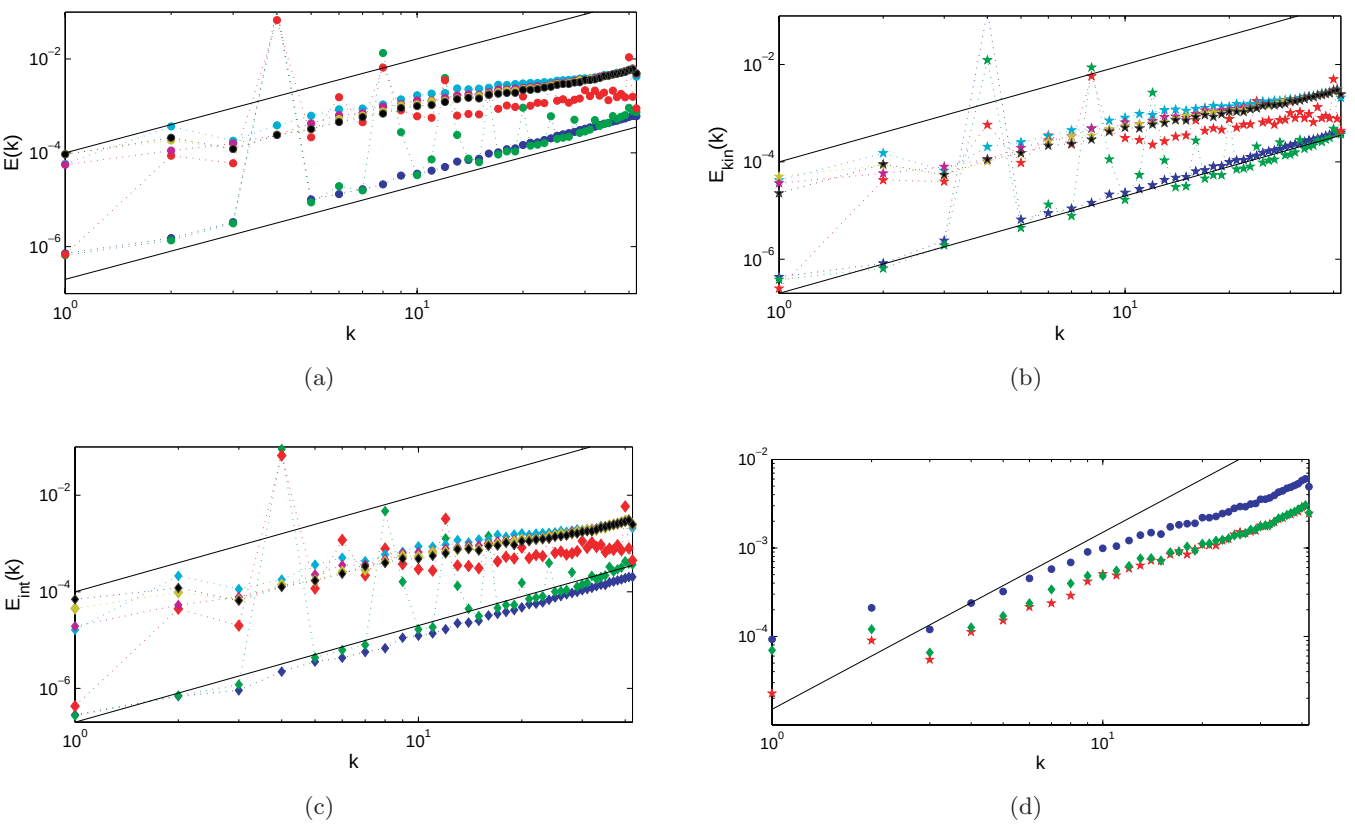

Fig. 2. Temporal evolution of compressible energy spectra (15)–(17). $t = 0$, 0.94, 6.19, 18.69, 31.19, 37.44, 43.69. Solid line represents a k^2 spectrum. (a) Total energy spectrum. (b) Kinetic energy spectrum. (c) Internal energy spectrum. (d) Total kinetic and internal energy spectra for $t = 43.69$.

Int. J. Bifurcation Chaos 2009.19:3445-3459. Downloaded from www.worldscientific.com by UNIVERSIDAD DE CHILE SISTEMA DE SERVICIOS DE INFORMACION Y BIBLIOTECAS (SISIB) on 03/20/13. For personal use only.

there is no clear k^2 law in the spectrum. This fact can be understood by noting that the k^2 law is a consequence of equipartition of energy which, in turn, requires that the total energy can be written as a sum of independent contributions from each mode, as in the incompressible case (4). In the compressible case, equipartition will not be obtained because of the non-Gaussian term (21).

An algorithm to generate such a general non-Gaussian absolute equilibria thus appears of practical interest for many applications such as the determination of eddy-viscosities or a two-fluid description. We now turn to this general problem.

4. New Algorithm to Generate Absolute Equilibrium

4.1. *Stochastic processes and stationary probability of Hamiltonian systems*

We want to construct a stochastic process with a probability distribution that converges to the stationary probability given by the Boltzmann weight. This can be done in a canonical way for any Hamiltonian system. Let $H(p_\mu, q^\mu)$ be a Hamiltonian with the corresponding canonicals equations

$$\dot{q}^\mu = \frac{\partial H}{\partial p_\mu}, \quad \dot{p}_\mu = -\frac{\partial H}{\partial q^\mu} \tag{24}$$

In what follows, we suppose the existence of a stable equilibrium point.

Let us first modify the equations by adding a dissipative term to the equation for $\dot{p}_\mu$

$$\dot{q}^\mu = \frac{\partial H}{\partial p_\mu} \tag{25}$$

$$\dot{p}_\mu = -\frac{\partial H}{\partial q^\mu} - \nu \frac{\partial H}{\partial p^\mu} \tag{26}$$

with $\nu > 0$. The dissipation introduced here is the most natural in a physical sense, as we will show later in the basic example of an oscillator. The dynamic has an evident Lyapunov functional given by the Hamiltonian H:

$$\frac{dH}{dt} = \frac{\partial H}{\partial q^\mu}\dot{q}^\mu + \frac{\partial H}{\partial p_\mu}\dot{p}_\mu = -\nu \frac{\partial H}{\partial p^\mu}\frac{\partial H}{\partial p_\mu} \leq 0, \tag{27}$$

therefore the system will converge to the stable equilibrium point.

Finally, let us introduce a white Gaussian forcing term. The Langevin equation, which completely defines the stochastic process, reads

$$\dot{q}^\mu = \frac{\partial H}{\partial p_\mu} \tag{28}$$

$$\dot{p}_\mu = -\frac{\partial H}{\partial q^\mu} - \nu \frac{\partial H}{\partial p^\mu} + \sqrt{2\eta\nu}\xi_\mu(t) \tag{29}$$

$$\langle \xi_\mu(t)\xi_\nu(t')\rangle = \delta_{\mu\nu}\delta(t-t'). \tag{30}$$

Note that when η and ν are small, the system (28)–(30) is a perturbation of the original Hamiltonian dynamics. In what follows, this system will be called the *damped Hamiltonian* method.

The Fokker–Planck equation for the evolution of the transition probability $P(p_\mu, q^\mu)$ of this process is [Langouche *et al.*, 1982; van Kampen, 2001]

$$\frac{\partial}{\partial t}P = -\frac{\partial}{\partial q^\mu}\left[\frac{\partial H}{\partial p_\mu}P\right] + \frac{\partial}{\partial p_\mu}\left[\frac{\partial H}{\partial q^\mu}P + \nu\frac{\partial H}{\partial p^\mu}P + \eta\nu\frac{\partial P}{\partial p^\mu}\right] \tag{31}$$

$$= \{H, P\} + \nu\frac{\partial}{\partial p_\mu}\left[\frac{\partial H}{\partial p^\mu}P + \eta\frac{\partial P}{\partial p^\mu}\right] \tag{32}$$

where $\{f, g\} = (\partial f/\partial q_\mu)(\partial g/\partial p^\mu) - (\partial f/\partial p_\mu)(\partial g/\partial q^\mu)$ is the Poisson bracket. As H is a conserved quantity of the original Eqs. (24), any function of a conserved quantity will vanish in the Poisson bracket and hence a stationary probability reads

$$P_{\rm st}(p_\mu, q^\mu) = \frac{1}{Z}e^{-\frac{1}{\eta}H(p_\mu, q^\mu)}. \tag{33}$$

Let us now remark that there exists another simple stochastic process which shares the same stationary probability. Its dynamics is given by gradient equations:

$$\dot{q}^\mu = -\nu\frac{\partial H}{\partial q^\mu} + \sqrt{2\eta\nu}\xi^1_\mu(t) \tag{34}$$

$$\dot{p}_\mu = -\nu\frac{\partial H}{\partial p^\mu} + \sqrt{2\eta\nu}\xi^2_\mu(t) \tag{35}$$

$$\langle \xi^s_\mu(t)\xi^{s'}_\nu(t')\rangle = \delta_{\mu\nu}\delta_{ss'}\delta(t-t') \tag{36}$$

however, we believe that the process (28)–(30) is of more physical and theoretical interest.

In the case of a Hamiltonian depending on fields, the generalization of Eqs. (28)–(30) are trivial replacing partial derivatives by functional derivatives and the $\delta_{\mu\nu}$ Kronecker delta in Eq. (30) by a Dirac delta. It is important to remark that absolute equilibria will formally lead, in this case, to

Int. J. Bifurcation Chaos 2009.19:3445-3459. Downloaded from www.worldscientific.com
by UNIVERSIDAD DE CHILE SISTEMA DE SERVICIOS DE INFORMACION Y BIBLIOTECAS (SISIB) on 03/20/13. For personal use only.

infinity energy solutions, therefore a UV cut-off must be understood leading to truncated equations in Fourier space.

4.1.1. *A simple example: Anharmonic oscillator*

Let us first consider the example of an anharmonic oscillator, the Hamiltonian for this system is $H(p,q) = (p^2/2m) + (mw^2q^2/2) + (\alpha q^4/4)$. The Langevin equation (28)–(30) reads

$$\dot{q} = \frac{1}{m}p \tag{37}$$

$$\dot{p} = -m\omega^2 q - \alpha q^3 - \frac{\nu}{m}p + \sqrt{2\eta\nu}\xi(t) \tag{38}$$

$$\langle \xi(t)\xi(t')\rangle = \delta(t-t'). \tag{39}$$

These equations can be rewritten as

$$m\ddot{q} = -m\omega^2 q - \alpha q^3 - \nu\dot{q} + \xi(t) \tag{40}$$

$$\langle \xi(t)\xi(t')\rangle = \delta(t-t') \tag{41}$$

and they are just the equations of a classical forced-damped anharmonic oscillator. In this sense, the dissipation introduced in (26) is very natural and with a simple physical interpretation.

4.2. *Hamiltonian formulation for general compressible fluids*

We have shown in Sec. 3 that irrotational compressible flows admit a Hamiltonian formulation. This can be easily extended to general compressible fluids. The equations that describe the dynamics of general inviscid fluids are the Euler and continuity equation for the velocity field $\mathbf{u}$

$$\partial_t \rho = -\nabla\cdot(\rho\mathbf{u}) \tag{42}$$

$$D_t\mathbf{u} = -\nabla w, \tag{43}$$

where D_t is the convective derivative defined as

$$D_t = \partial_t + \mathbf{u}\cdot\nabla,$$

ρ is the density and w is the enthalpy for unit of mass. For isoentropic fluids the enthalpy is related to the pressure field p by

$$\nabla w = \frac{\nabla p}{\rho}.$$

For the purposes of this work we assume a barotropic dynamics, hence the pressure field has functional dependence only in ρ. We also suppose that the density field is approximately uniform throughout the fluid and therefore the dependence in ρ of w can be written as

$$w(\rho) = c^2(\rho - 1)$$

where c is the speed of sound for a unit density fluid.

It is well known that it is possible to find a variational principle for Eqs. (42) and (43) with the help of the *Weber–Clebsch Transformation* [Mobbs, 1982]

$$\mathbf{u} = \sum_{i=1}^{3}\lambda^i\nabla\mu^i + \nabla\phi\,, \tag{44}$$

here, we write the velocity field as a function of the scalar fields $\lambda^i(x,t)$, $\mu^i(x,t)$ and $\phi(x,t)$.

In order to show explicitly the Hamiltonian structure of Eqs. (42) and (43) we redefine

$$\tilde{\lambda}^i = \rho\lambda^i \tag{45}$$

and with this representation of $\mathbf{u}$ we define the Lagrangian

$$L = \int dx^3dt\left(\rho\partial_t\phi + \sum_{i=1}^{3}\tilde{\lambda}^i\partial_t\mu^i + \mathcal{H}\right),$$

where $\mathcal{H}$ is the Hamiltonian density

$$\mathcal{H} = \rho\frac{\mathbf{u}^2}{2} + \varepsilon(\rho)$$

and $\varepsilon(\rho)$ is the internal energy (9) which is related to w [Landau & Lifchitz, 1971] by the relation

$$\rho\frac{\partial\varepsilon}{\partial\rho} = \varepsilon + p = \rho w. \tag{46}$$

With this choice of variables, $\tilde{\lambda}^i, \tilde{\mu}^i$ and $\hat{\rho}_{\mathbf{k}}, \hat{\phi}_{\mathbf{k}}$ are now conjugate variables. The corresponding canonical equations are then

$$\partial_t\rho = \frac{\delta\mathcal{H}}{\delta\phi} = -\nabla\cdot(\rho\mathbf{u}) \tag{47}$$

$$\partial_t\phi = -\frac{\delta\mathcal{H}}{\delta\rho} = -\mathbf{u}\cdot\nabla\phi + \frac{\mathbf{u}^2}{2} - \frac{\partial\varepsilon}{\partial\rho} \tag{48}$$

$$\partial_t\tilde{\lambda}^i = \frac{\delta\mathcal{H}}{\delta\mu^i} = -\nabla\cdot(\mathbf{u}\tilde{\lambda}^i) \tag{49}$$

$$\partial_t\mu^i = -\frac{\delta\mathcal{H}}{\delta\tilde{\lambda}^i} = -\mathbf{u}\cdot\nabla\mu^i. \tag{50}$$

Let us remark that Eq. (47) is the continuity equation (42) and that Eq. (48) is the Bernoulli equation, with an extra advective term.

Int. J. Bifurcation Chaos 2009.19:3445-3459. Downloaded from www.worldscientific.com by UNIVERSIDAD DE CHILE SISTEMA DE SERVICIOS DE INFORMACION Y BIBLIOTECAS (SISIB) on 03/20/13. For personal use only.

In order to recover the Euler equation (43) from Eqs. (47)–(50) note that reintroducing the definition (45) of $\tilde{\lambda}^i$ in Eq. (49) and using Eq. (47) we obtain $\partial_t \lambda^i = -\mathbf{u}\cdot\nabla\lambda^i$. Computing then $D_t\mathbf{u}$ using the definition (44), the identity $[\nabla, D_t] \equiv (\nabla\mathbf{u})\cdot\nabla$ and thermodynamic relation (46), Eq. (42) is obtained after some simple algebra.

The general system (47)–(50) admits two simple limits. First, when ρ is constant, the flow is incompressible and the dynamics reduces to equations of motion for λ^i and μ^i. In this case, there is no need to independently solve for ϕ, because this field is determined by the incompressibility condition $\nabla\cdot\mathbf{u} = 0$. A second simple case is when the flow is compressible and irrotational. As the velocity is a purely potential flow, the Clebsch variables λ^i, μ^i vanish and the dynamics reduces to equations of motion for the fields ρ and ϕ only, as in Sec. 3.

4.3. *Langevin equation converging to absolute equilibrium*

Our new algorithms are obtained by inserting within the Langevin equations (28)–(30) the Hamiltonian corresponding to the two particular cases of the preceding subsection.

4.3.1. *Incompressible flows*

When ρ is constant, the Hamiltonian (46) reduces to

$$\mathcal{H} = \int d^3x\, \frac{1}{2}(\lambda^i\nabla\mu^i - \nabla\phi)^2 \tag{51}$$

with the corresponding Langevin equation:

$$\frac{\partial\lambda^i}{\partial t} = -\mathbf{u}\cdot\nabla\lambda^i \tag{52}$$

$$\frac{\partial\mu^i}{\partial t} = -\mathbf{u}\cdot\nabla\mu^i + \nu\,\mathbf{u}\cdot\nabla\lambda^i + \sqrt{2\eta\nu}\,\xi^i(x,t) \tag{53}$$

$$\nabla\cdot\mathbf{u} = 0 \tag{54}$$

$$\langle\xi^i(x,t)\xi^j(x',t')\rangle = \delta_{ij}\delta^3(x-x')\delta(t-t') \tag{55}$$

Note that the stationary probability is in some way similar to that of $\lambda-\phi^4$ theory in the Clebsch variables. Although the velocity $\mathbf{v}$ must have an equipartition k^2 spectrum (in 3D), the statistical properties of the Clebsch pairs are not at all trivial.

4.3.2. *Irrotational flows*

In the compressible irrotational case where only the fields ρ and ϕ are not zero, we recover the Hamiltonian (12) and the corresponding Langevin equation reads:

$$\frac{\partial\rho}{\partial t} = -\nabla\cdot(\rho\nabla\phi) \tag{56}$$

$$\frac{\partial\phi}{\partial t} = -\frac{1}{2}(\nabla\phi)^2 - \frac{\partial\epsilon}{\partial\rho}(\rho) + \nu\nabla\cdot(\rho\nabla\phi) + \sqrt{2\eta\nu}\,\xi(x,t) \tag{57}$$

$$\langle\xi(x,t)\xi(x',t')\rangle = \delta^3(x-x')\delta(t-t'). \tag{58}$$

Note that when ρ is a small fluctuation around a homogeneous value ρ_0 given by the minimum of $\varepsilon(\rho)$, the dissipation looks like a diffusion term and taking the gradient in Eq. (57), we obtain a Navier–Stokes like equation.

Another important property of this Langevin Eqs. (56)–(58) is that the mean value of ρ (average over space and realization of the process) is conserved as in the original Hamiltonian dynamics (6) and (7). This property is not preserved in the gradient dynamics (35) and (36). In this case, it follows directly from Eq. (35), and the Hamiltonian (12), that the dynamics of $\langle\rho\rangle$ is given by

$$\frac{\partial}{\partial t}\langle\rho\rangle = -\frac{1}{2}\langle\nabla\phi^2\rangle - \left\langle\frac{\partial\epsilon}{\partial\rho}\right\rangle$$

and hence, using the internal energy (9) the stationary value of $\langle\rho\rangle$ is

$$\langle\rho\rangle_{\rm st} = 1 - \frac{1}{2c^2}\langle\nabla\phi^2\rangle_{\rm st}. \tag{59}$$

Remark that this usual equation of state (9) can lead to high values of η [see Eq. (33)] to negative values of ρ. This non-physical situation can be avoided by changing the equation of state to one physically more compatible with the dynamics of high amplitude waves, considering for instance, terms of order $O((\rho-1)^4)$ in (9).

5. Numerical Validation

5.1. *Incompressible rotational flows*

We now proceed to validate our new algorithm in the well-known test case of incompressible fluids. Although the Hamiltonian (51) is not quadratic, the velocity $\mathbf{u}$ must be Gaussian and therefore the energy spectrum of the velocity must follow a k^2 law.

Int. J. Bifurcation Chaos 2009.19:3445-3459. Downloaded from www.worldscientific.com
by UNIVERSIDAD DE CHILE SISTEMA DE SERVICIOS DE INFORMACION Y BIBLIOTECAS (SISIB) on 03/20/13. For personal use only.

In the case of absolute equilibria of incompressible fluids, there are only two independent components of velocity due to the divergence free condition (54). It can be shown [Orszag, 1970; Cichowlas, 2005] that the second order moment of a Fourier mode is

$$\langle \hat{u}_\mu(\mathbf{k},t)\hat{u}_\nu(-\mathbf{k},t)\rangle = \eta\left(\delta_{\mu\nu} - \frac{k_\mu k_\nu}{k^2}\right) = \eta P_{\mu\nu}(\mathbf{k}), \quad (60)$$

and therefore the kinetic energy $\mathcal{H}$ is obtained from Eq. (60)

$$\mathcal{H} = \sum_{|k_\alpha|\le k_{\max}} \frac{1}{2}\langle \hat{u}_\alpha(\mathbf{k},t)\hat{u}_\alpha(-\mathbf{k},t)\rangle = \frac{\eta}{2}\sum_{|k_\alpha|\le k_{\max}} P_{\alpha\alpha}(\mathbf{k}). \quad (61)$$

As $P_{\alpha\alpha} = 2$ then $\mathcal{H} = \eta\mathcal{N}$ where $\mathcal{N}$ is the number of degrees of freedom.

We perform the numerical integration of (52)–(55) using a standard pseudo-spectral method with a Galerkin truncation at the mode $k_{\max}$ with the 2/3 rule.

In Fig. 3 we plot temporal evolution of the total energy of the velocity field for the gradient and damped Hamiltonian method. We set $\nu = 1$ for all present simulations. We can see a faster convergence to the stationary value of the energy in the gradient method.

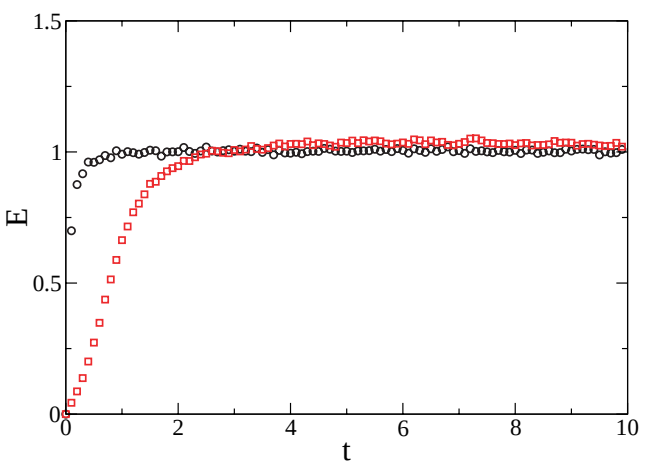

Fig. 3. Temporal evolution of the total energy (51) of the velocity field for the gradient and damped Hamiltonian method (○ and □) for simulations made with a resolution of 48^3 and $\nu = 1$.

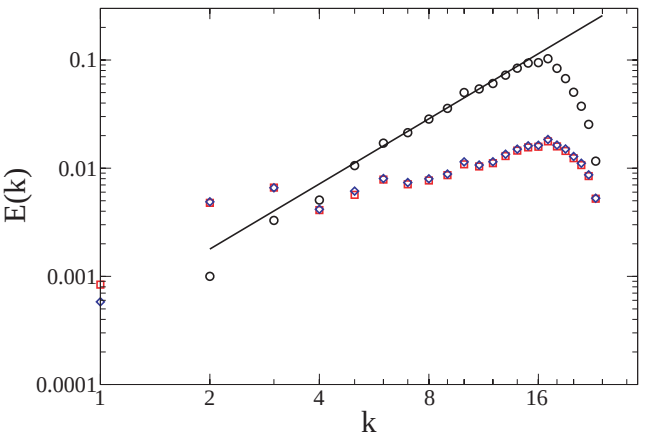

Fig. 4. Energy spectrum for the velocity, λ and μ fields (○, □ and ◇) of the gradient case for a simulation with a resolution 48^3. The continuous line represents an ideal k^2 spectrum.

As usual, we define the energy spectrum of λ and μ by averaging on spherical shells

$$E_\lambda(k,t) = \frac{1}{2}\sum_{k-\Delta k/2<|\mathbf{k}'|<k+\Delta k/2} |\hat{\lambda}_{\mathbf{k}'}|^2(t) \quad (62)$$

$$E_\mu(k,t) = \frac{1}{2}\sum_{k-\Delta k/2<|\mathbf{k}'|<k+\Delta k/2} |\hat{\mu}_{\mathbf{k}'}|^2(t), \quad (63)$$

and the averaged spectra over a set of a hundred realizations of the process is shown in Fig. 4. We can see a good agreement of the velocity spectrum with the equipartition scaling $\sim k^2$. We remark that scaling of λ and μ fields appears to obey scaling laws that seem different from k^2.

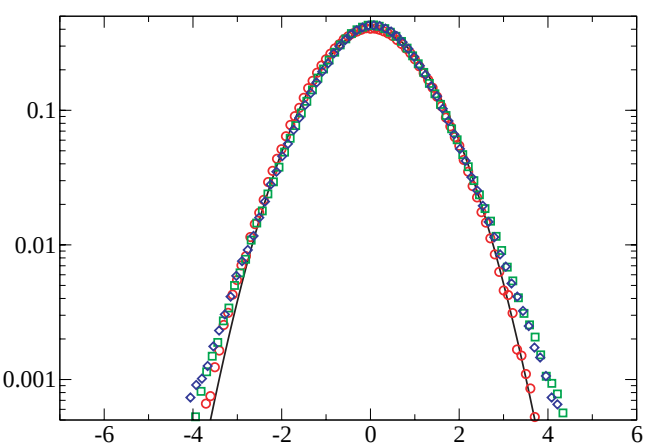

Fig. 5. Histogram for the x component of the velocity, λ and μ fields (○, □ and ◇) for the damped Hamiltonian case from a simulation made with a resolution of 48^3. The continuous line represents an ideal Gaussian distribution for the velocity.

Int. J. Bifurcation Chaos 2009.19:3445-3459. Downloaded from www.worldscientific.com
by UNIVERSIDAD DE CHILE SISTEMA DE SERVICIOS DE INFORMACION Y BIBLIOTECAS (SISIB) on 03/20/13. For personal use only.

Finally, a normalized histogram of λ, μ and one component of $\mathbf{u}$ are plotted in Fig. 5. It is manifest in the figure that the statistics of the velocity field are approximatively Gaussian (compare the tails with those of the λ and μ fields). We, therefore, conclude that our new algorithm is validated in the sense that it reproduces the Gaussian statistics in the incompressible limit.

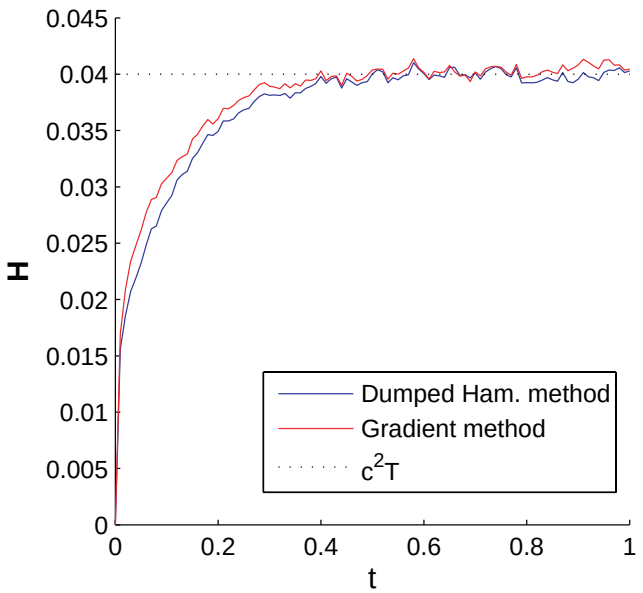

(a)

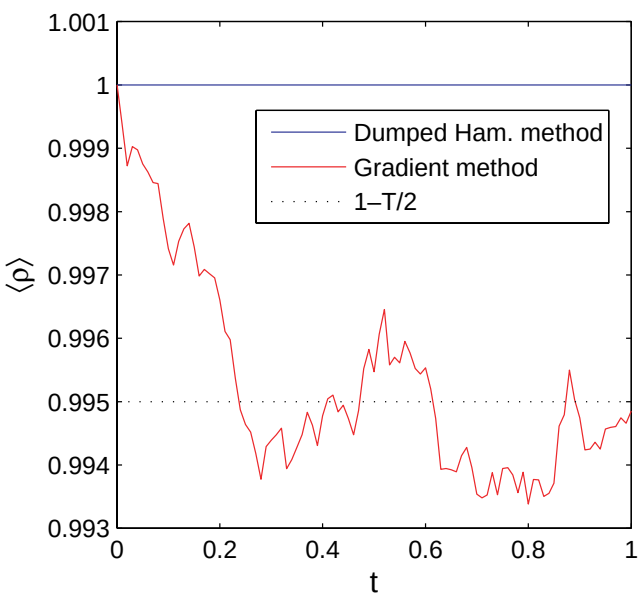

(b)

Fig. 6. (a) Convergence of compressible energy (12). (b) Plot of $\langle\rho\rangle$. Straight line: Gaussian value, $T = 0.01$.

5.2. *Compressible irrotational flows*

In order to validate our new algorithm in the compressible case (see Sec. 4.3.2) we will check that it generates data that is a statistical stationary solution of the original equation of motion and that it reproduces the spectrum obtained by direct relaxation in Sec. 3.

At low values of η, the distribution of ρ, ϕ is almost Gaussian and the predicted value of relevant quantities using the Hamiltonian (12) and the stationary probability density (33) read

$$\langle(\rho-1)^2\rangle = \frac{\mathcal{N}\eta}{c^2}, \quad \langle(\nabla\phi)^2\rangle = \mathcal{N}\eta, \quad \langle H\rangle = \mathcal{N}\eta$$

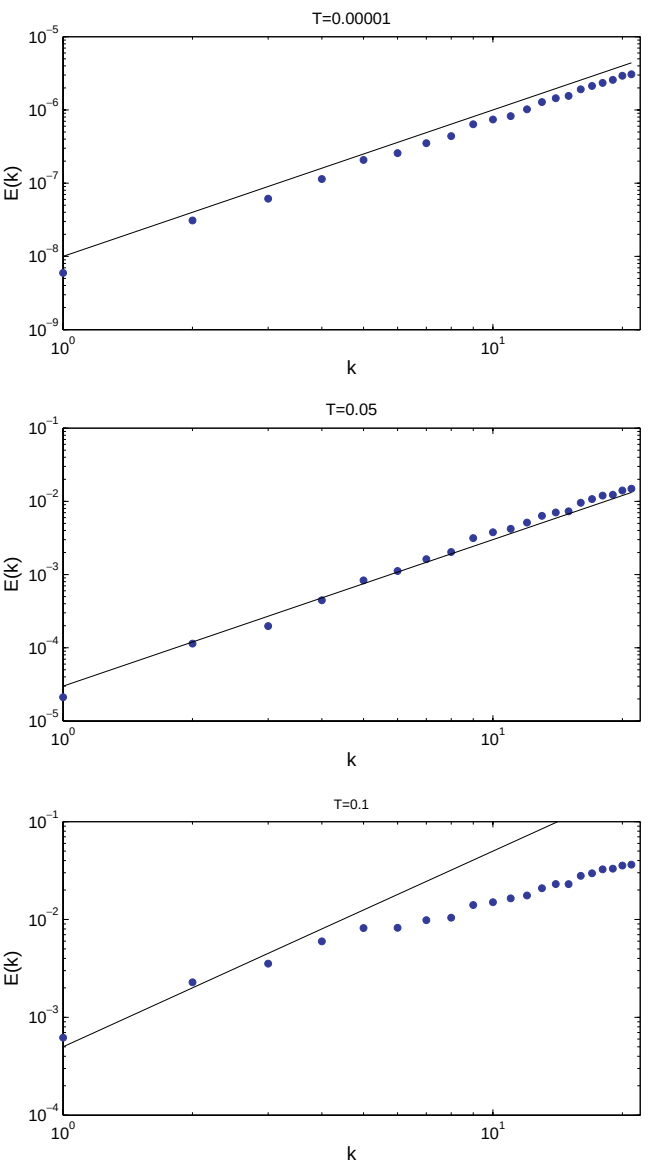

Fig. 7. Total compressible energy spectra for $T = 0.0001$, 0.05, 0.1.

Int. J. Bifurcation Chaos 2009.19:3445-3459. Downloaded from www.worldscientific.com
by UNIVERSIDAD DE CHILE SISTEMA DE SERVICIOS DE INFORMACION Y BIBLIOTECAS (SISIB) on 03/20/13. For personal use only.

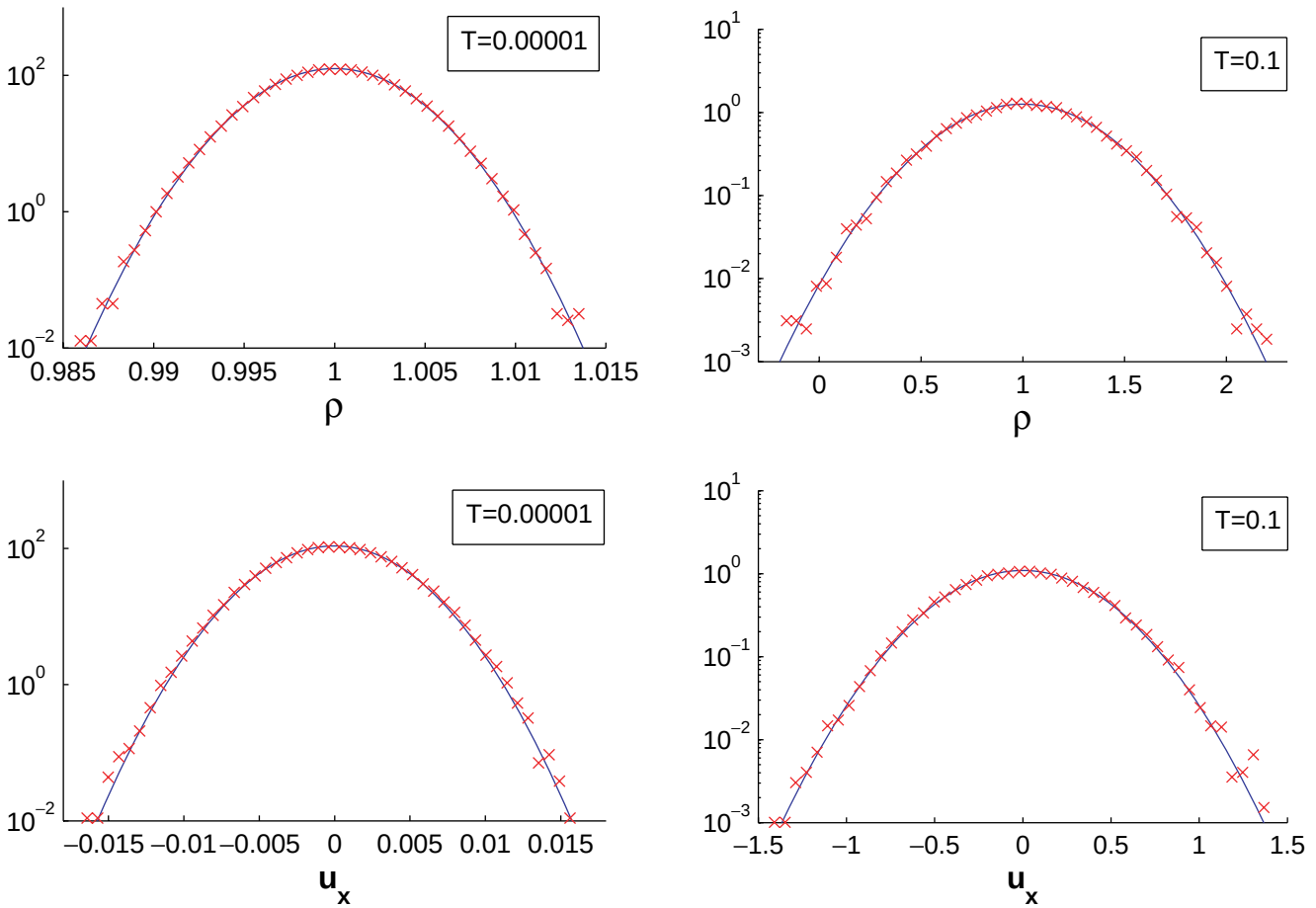

Fig. 8. Histograms of ρ and u_x obtained from Eqs. (56)–(58).

where $\mathcal{N}$ is the number of degrees of freedom. We redefine

$$\frac{1}{\eta} \equiv \beta = \frac{\mathcal{N}}{c^2 T}.$$

In what follows, we vary T in the numerics from $T = 0.00001$ to $T = 0.1$ using 64^3 Fourier modes and we set $c = 2$ and $\nu = 1$, using the usual equation of state (9). We start from the homogenous and minimum energy solution $\rho(x, t = 0) = 1, \phi(x, t = 0) = 0$ and the integration of Eqs. (56)–(58) is performed until convergence is achieved.

Figure 6 shows the convergence of the energy using both methods (56)–(58) and (35)–(36) at $T = 0.01$. We checked that the final data is a statistical stationary solution of the continuity and Bernouilli equations (6)–(8) (data not shown). Note that the convergence of the gradient method is not much faster than that of the damped Hamiltonian method. In this gradient case, the spatial average of the density fluctuates around the stationary value given by Eq. (59) $\langle\rho\rangle_{\text{st}} = 1 - (1/2)T$.

Figure 7 displays the energy spectra (17) computed on the time-converged solution of Eqs. (56)–(58), at different values of the temperature. Note that at high temperature the k^2 law is not manifest in the spectrum. This spectrum should be compared with those of Fig. 2(d) that were obtained by the relaxation of the original dynamics. The similarity of the spectra confirms that equipartition is not obtained in the compressible case because of the non-Gaussian term (21).

In Fig. 8, we show an histogram of $u_x = \partial_x \phi$ and ρ together with the Gaussian predictions, we see that they seem to remain Gaussian even for the highest values of $T = 0.1$. There are some low probability events with $\rho < 0$ and higher values of T will lead to more negatives values of ρ.

Note, however, that the total distribution is non-Gaussian. Indeed, if it remained Gaussian at higher values of T, the correlation between $\nabla\phi^2$ and $\rho - 1$ will vanish and this it is not observed in Fig. 9 where the histograms of $z = (\rho - 1)\nabla\phi^2$

Int. J. Bifurcation Chaos 2009.19:3445-3459. Downloaded from www.worldscientific.com
by UNIVERSIDAD DE CHILE SISTEMA DE SERVICIOS DE INFORMACION Y BIBLIOTECAS (SISIB) on 03/20/13. For personal use only.

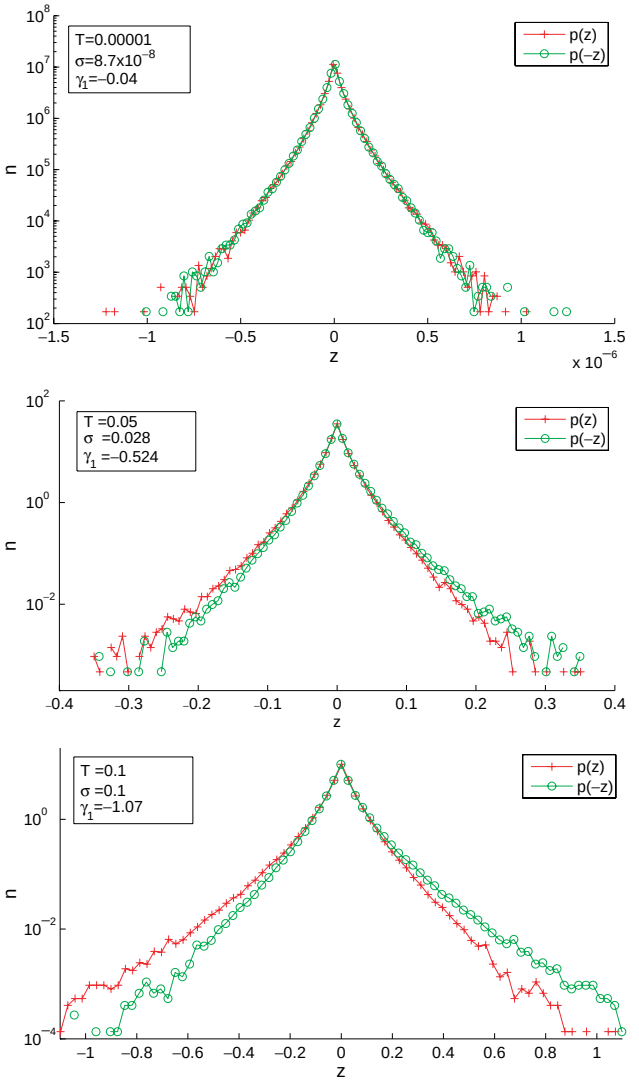

Fig. 9. Histograms of $z = (\rho - 1)\nabla\phi^2$ and $-z$ for $T = 0.0001, 0.05, 0.1$. In the insert the standard deviation σ and skewness γ_1.

and $-z$ are shown. Note that for the lowest temperature Fig. 9(a), the standard deviation is extremely small, the pdf is symmetric and all points are heavily concentrated around $z = 0$, the correlation between $\nabla\phi^2$ and $\rho - 1$ is thus completely negligible. However, for higher temperatures Figs. 9(b) and 9(c), the pdf becomes asymmetrical and the skewness $\gamma_1 = \mu_3/\sigma^3$, where μ_3 is the third moment about the mean and σ is the standard deviation, are of order one.

6. Relaxation of Initial Data with Temperature Oscillation

Let us now consider a practical application of our algorithm. We want to study how truncated irrotational compressible flows relax to the equilibrium. A big difference with the incompressible case studied in [Cichowlas *et al.*, 2005; Krstulovic & Brachet, 2008] is that waves can appear as the principal mechanism of homogenization as in the Landau two-fluid model for superfluids [Landau & Lifchitz, 1971] where the temperature waves propagate at a *second sound* speed slower than pressure waves. Indeed, Larraza and Putterman [1986] argued that, in a nonlinear medium pumped with energy sufficiently far from equilibrium the wave turbulence can support a transition from diffusive to propagative energy transport that bears deep similarities to second sound in Helium.

In this section we give preliminary results that seem to suggest that such a behavior is present. However, these results need to be confirmed and further studies will be presented in a future publication.

In order to check for the presence of this mechanism, we need to reduce the emission of (first) sound that would trivially generate propagative dynamics. To wit, we prepare an initial condition with constant pressure. In compressible flows, the pressure appears in the δ_{ij} contribution of the momentum flux density tensor

$$\Pi_{ij} = \rho u_i u_j + \delta_{ij} p \tag{64}$$

where for the internal energy (9), the pressure simply reads $p = (c^2/2)\rho^2$.

Consider now fluctuating fields replacing $\rho \to \rho + \rho'$ and $u_i \to u_i + u'_i$, where the quantities with primes are of zero mean and with the obvious correspondence $\widehat{u}_{j\mathbf{k}} = ik_j\hat{\phi}_{\mathbf{k}}$ and $\widehat{u}_{j\mathbf{k}} = ik_j\hat{\phi}'_{\mathbf{k}}$. The mean value of Π_{ij} over the different realization then reads

$$\langle\Pi_{ij}\rangle = \rho u_i u_j + \langle\rho u'_i\rangle u_j + \langle\rho u'_j\rangle u_i + \rho\langle u'_i u'_j\rangle + \langle\rho' u'_i u'_j\rangle + \delta_{ij}\frac{c^2}{2}(\rho^2 + \langle\rho'^2\rangle). \tag{65}$$

If we assume isotropy we obtain

$$\langle u'_i u'_j\rangle = \frac{\delta_{ij}}{d}\langle\mathbf{u}'^2\rangle \quad \langle\rho' u'_i u'_j\rangle = \frac{\delta_{ij}}{d}\langle\rho'\mathbf{u}'^2\rangle,$$

where d is the dimension of the space. The δ_{ij} contribution part of $\langle\Pi_{ij}\rangle$ is then

$$\tilde{p} = \frac{c^2}{2}\rho^2 + \frac{c^2}{2}\langle\rho'^2\rangle + \frac{\rho}{d}\langle\mathbf{u}'^2\rangle + \frac{1}{d}\langle\rho'\mathbf{u}'^2\rangle. \tag{66}$$

Consider that the small fluctuations of the fields are approximatively given by the stationary Gaussian pdf $P\{\hat{\rho}_{\mathbf{k}}, \hat{\phi}_{\mathbf{k}}\} \sim e^{-\beta\tilde{H}}$ where $\beta = \mathcal{N}/(c^2 T)$ and

Int. J. Bifurcation Chaos 2009.19:3445-3459. Downloaded from www.worldscientific.com
by UNIVERSIDAD DE CHILE SISTEMA DE SERVICIOS DE INFORMACION Y BIBLIOTECAS (SISIB) on 03/20/13. For personal use only.

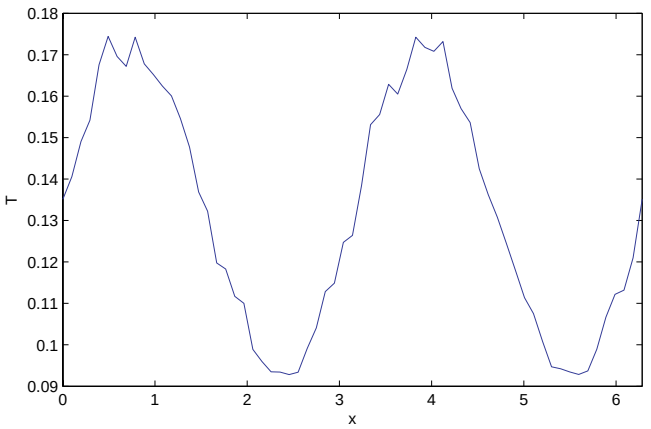

(a1)

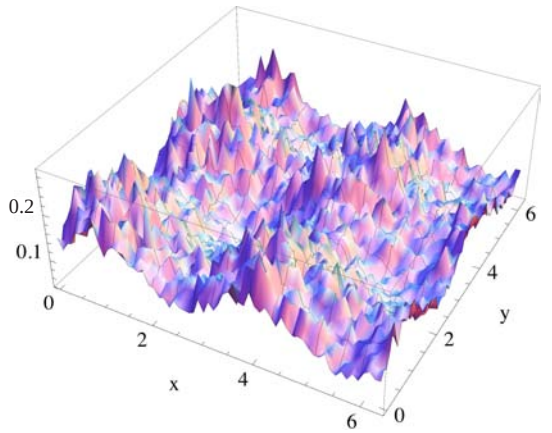

(b1)

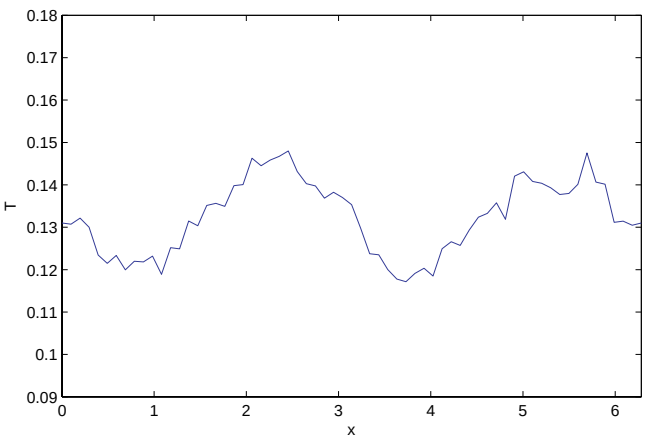

(a2)

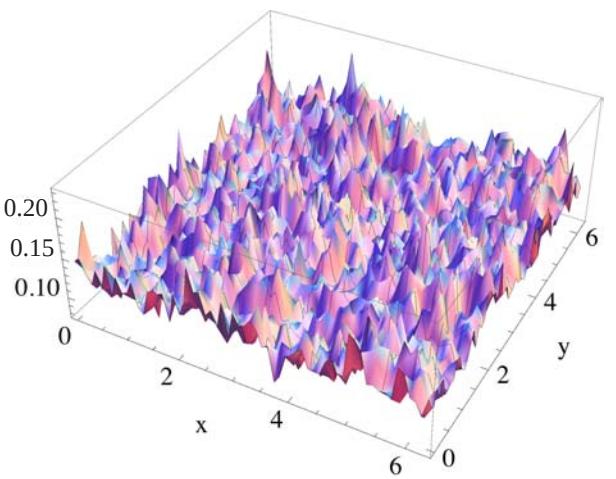

(b2)

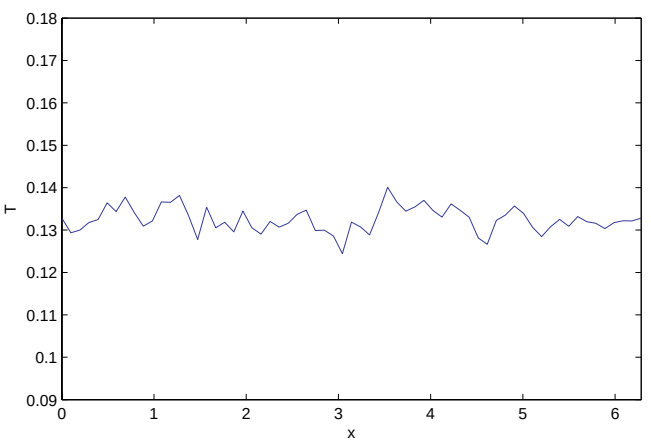

(a3)

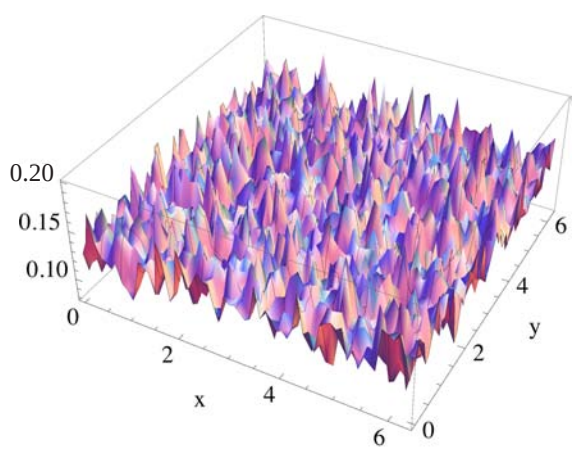

(b3)

Fig. 10. Temporal evolution of the spatially averaged temperatures over z, y [(a1)–(a3)] and z [(b1)–(b3)] corresponding to initial data (72) at $t = 0$, 1.4, 2.8.

Int. J. Bifurcation Chaos 2009.19:3445-3459. Downloaded from www.worldscientific.com by UNIVERSIDAD DE CHILE SISTEMA DE SERVICIOS DE INFORMACION Y BIBLIOTECAS (SISIB) on 03/20/13. For personal use only.

$\tilde{H} = H_{\mathrm{G}} - \mu Q$ is defined in Eqs. (10), (11) and (20). After a straightforward calculation, it is possible to show that

$$\langle \rho \rangle = 1 + \frac{\mu}{c^2} \tag{67}$$

$$\langle \mathbf{u}'^2 \rangle = \frac{c^2}{1 + \mu/c^2} \langle \rho'^2 \rangle = \frac{c^2}{1 + \mu/c^2} T \tag{68}$$

$$\langle H \rangle = \frac{c^2}{2} \frac{2 + \mu/c^2}{1 + \mu/c^2} T. \tag{69}$$

Then $\tilde{p}$ reads at leading order

$$\tilde{p} = \frac{c^2}{2} \left(1 + \frac{\mu}{c^2}\right)^2 + \frac{d+2}{2d} c^2 T. \tag{70}$$

Thus setting

$$\frac{\mu}{c^2} = -1 + \sqrt{1 - T(d+2)/d} \tag{71}$$

yields a constant pressure $\tilde{p} = c^2/2$.

Consider now T and $\mu(T)$ given by Eq. (71) that are slow space variable functions where T has a sinus modulation

$$T(x, y, z) = T_0 (1 + \epsilon (\sin(2x) + \sin(2y) + \sin(2z))). \tag{72}$$

We set in the present numeric simulation $T_0 = 0.03$ and $\epsilon = 0.3$. The temporal evolution of the spatially averaged temperatures over z, y and z is shown in Fig. 10. Note that there is a fast decay of the amplitude of the modulation as predicted in [Larraza & Putterman, 1986] for compressible flows. Remark that at $t = 1.4$ the phase of the wave changed in a factor π, that gives a rough estimate of the oscillation frequency $\omega_T = \pi/1.4 = 2.244$. This value is smaller than the frequency of first sound $\omega = ck = 4$.

The presence of an oscillating behavior in this constant pressure variable temperature relaxation strongly suggests the existence of second sound. However, this interesting behavior needs to be confirmed and studied in more detail. In the future, we will investigate the relaxation of full, first and second sound perturbations.

7. Conclusion

Our new method to generate absolute equilibrium of spectrally truncated compressible flows has been shown to reproduce the well-known Gaussian results in the incompressible limit. The irrotational compressible absolute equilibrium case was characterized and the distribution was shown to be non-Gaussian. The spectrum were found not to obey a k^2 scaling, just as those obtained directly by relaxation of the original dynamics. Finally, oscillating behavior in constant pressure variable temperature relaxation was obtained, suggesting the presence of second sound.

Acknowledgments

We acknowledge support from an ECOS/CONICYT action and one of the authors (ET) is grateful to the Project ACT 15 of CONICYT, Chile. The computations were carried out at IDRIS (CNRS).

References

Bos, W. J. T. & Bertoglio, J.-P. [2006] "Dynamics of spectrally truncated inviscid turbulence," *Phys. Fluids* **18**, 071701.

Cichowlas, C. [2005] *Equation d'Euler tronquée: de la dynamique des singularités complexes à la relaxation turbulente*, Université Pierre et Marie Curie — Paris VI.

Cichowlas, C., Bonaïti, P., Debbasch, F. & Brachet, M. E. [2005] "Effective dissipation and turbulence in spectrally truncated Euler flows," *Phys. Rev. Lett.* **95**, 26.

Connaughton, C., Josserand, C., Picozzi, A., Pomeau, Y. & Rica, S. [2005] "Condensation of classical nonlinear waves," *Phys. Rev. Lett.* **95**, 26.

Fermi, E., Pasta, J. & Ulam, S. [1955] *Studies of Nonlinear Problems. I*, Los Alamos Report LA 1940.

Frisch, U., Kurien, S., Pandit, R., Pauls, W., Ray, S. S., Wirth, A. & Zhu, J.-Z. [2008] "Hyperviscosity, Galerkin truncation and bottlenecks in turbulence," *Phys. Rev. Lett.* **101**, 144501.

Gottlieb, D. & Orszag, S. A. [1977] *Numerical Analysis of Spectral Methods* (SIAM, Philadelphia).

Kraichnan, R. H. [1973] "Helical turbulence and absolute equilibrium," *J. Fluid Mech.* **59**, 745–752.

Krstulovic, G. & Brachet, M. E. [2008] "Two-fluid model of the truncated Euler equations," *Physica D* **237**, 2015–2019.

Krstulovic, G., Mininni, P. D., Brachet, M. E. & Pouquet, A. [2009] "Cascades, thermalization and eddy viscosity in helical Galerkin truncated Euler flows," *Phys. Rev. E* **79**, 056304.

Landau, L. & Lifchitz, E. [1971] *Mécanique des Fluides* (MIR).

Langouche, F., Roekaerts, D. & Tirapegui, E. [1982] *Functional Integration and Semiclassical Expansions* (D. Reidel Pub. Co. Hingham).

Larraza, A. & Putterman, S. J. [1986] "Second sound in wave turbulence: A clue to the cause of anomalous plasma diffusivity," *Phys. Rev. Lett.* **57**, 22.

Lee, T. D. [1952] "On some statistical properties of hydrodynamical and magneto-hydrodynamical fields," *Quart. J. Appl. Math.* **10**, 69.

Mobbs, S. D. [1982] "Variational principles for perfect and dissipative fluid flows," *Proc. R. Soc. Lond. A* **381**, 457–468.

Orszag, S. A. [1970] "Analytical theories of turbulence," *J. Fluid Mech.* **41**, 363.

Orszag, S. A. [1977] *Statistical Theory of Turbulence*, Les Houches 1973: Fluid Dynamics, eds. Balian, R. & Peube, J. L. (Gordon and Breach, NY).

Putterlman, S. J. & Roberts, P. H. [1982] "Non-linear hydrodynamics and a one fluid theory of superfluid HE-4," *Phys. Lett. A* **89**, 444–447.

Putterman, S. J. & Roberts, P. H. [1983] "Classical non-linear waves in dispersive nonlocal media, and the theory of superfluidity," *Physica A* **117**, 369–397.

van Kampen, N. G. [2001] *Stochastic Processes in Physics and Chemistry* (North-Holland).

Int. J. Bifurcation Chaos 2009.19:3445-3459. Downloaded from www.worldscientific.com
by UNIVERSIDAD DE CHILE SISTEMA DE SERVICIOS DE INFORMACION Y BIBLIOTECAS (SISIB) on 03/20/13. For personal use only.